Development of a silicon-based quantum cellular automata cell

M. Mitic*, M.C. Cassidy*, K.D. Petersson*, E. Gauja*, R.P. Starrett*, R. Brenner*,
C. Yang**, D.N. Jamieson**, R.G. Clark* and A.S. Dzurak*

* Centre for Quantum Computer Technology, Schools of Electrical Engineering and Physics,
University of New South Wales, NSW 2052, AUSTRALIA, z2255597@student.unsw.edu.au
** Centre for Quantum Computer Technology, School of Physics,
University of Melbourne, VIC 3010, AUSTRALIA

ABSTRACT

We report on the development of a phosphorus-doped silicon quantum cellular automata (QCA) unit cell. The device studied consists of two pairs of metallic dots, separated from source and drain reservoirs by tunnel barriers. The metallic regions were formed by low-energy (14 keV) phosphorous ion implantation through a nanoscale mask defined using electron beam lithography. Metallic gates used to control the electrostatic potential of the dots, along with Al-AlO_x single-electron transistors used for non-invasive QCA cell state-readout, were fabricated on the surface of this structure, isolated from the dots and reservoirs by a 5nm thick layer of SiO_2. The device was operated in a dilution refrigerator at a base temperature of 50 mK. Preliminary experimental data reveals evidence of capacitive coupling between the two implanted half-cells, a very important result leading the way towards the demonstration of a fully functional phosphorous doped silicon QCA.

Keywords: quantum cellular automata, QCA, nanolithography, electron beam lithography, ion implantation.

1 INTRODUCTION

During the last few decades, the microelectronics industry has continued to scale down the size of electronic devices in order to achieve higher speeds and denser CMOS circuit arrays. This trend will eventually be limited by fundamental processes, such as quantum tunneling in ultra-small devices, and unacceptably high levels of power density. Quantum cellular automata [1] (QCA) is a revolutionary paradigm in computation based on single electron charge control, providing potential solutions to these critical problems. The basic building block of a QCA system is a cell made up of four quantum or metallic dots coupled by tunnel barriers (Fig. 1a). If two electrons are added to the cell, their mutual electrostatic repulsion forces them to occupy diagonal sites, giving rise to two possible polarization states of the cell. If properly assembled, two dimensional arrays of such QCA cells can be used to form logic gates and memory storage devices [1].

To date, QCA cells have been experimentally demonstrated using Al metallic dots [2] and magnetic dot systems [3]. Promising results have also been achieved in GaAs quantum dot systems [4]. In this paper we report on the fabrication and preliminary experimental measurements in the course of development of an ion-implanted phosphorus-doped silicon QCA cell. Some important advantages of this system include compatibility with Si-CMOS technologies and a great potential for cell size reduction down to single donors, leading to fast (sub-ns), low-power high-density computing devices [5].

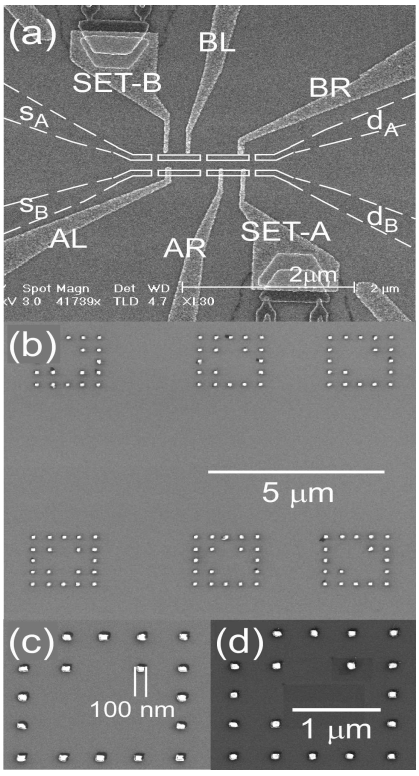

Fig. 1. Scanning electron micrographs: (a) completed device with the implanted QCA cell marked using dashed white lines; (b) array of registration markers used to align surface electrodes to buried n^+ regions; (c) registration marker before the RTA; (d) registration marker after the RTA.

An SEM image of the complete Si:P QCA cell, studied in this paper, is shown in Fig.1 a. It consists of two implanted double-dots with leads (half-cells), marked using dashed white lines in Fig. 1a. Each half-cell consists of two metallically doped phosphorous islands, tunnel-coupled to each other and to electron reservoirs (leads) labeled in Fig. 1a as s_A, d_A (s_B, d_B) for half-cell A (half-cell B). Control of electron number occupancy on the implanted islands, defined as $\{n_A, m_A\}$ and $\{n_B, m_B\}$ for the two half-cells, was achieved using four surface gates, labeled as AL, AR, BL and BR in Fig. 1a, while the two Al-AlO_x single electron transistors (SETs) were used to provide non-invasive charge-state readout [6], as previously demonstrated in Si:P double dots [7]. Accurate alignment throughout the fabrication process was essential and it was achieved using specially designed registration markers, shown in Fig. 1 b-d.

2 FABRICATION

The devices were fabricated on a near-intrinsic ($n < 10^{12}$ cm^{-3}) n-type silicon wafer of resistivity greater than 5 kΩ cm. Firstly, the n^+ ohmic contacts for the source and drain leads (labeled as s_A, d_A, s_B and d_B in Fig. 1a) were defined by phosphorous contact diffusion at 950C°, through a photo-lithographically defined *oxide* mask (Fig. 2a). Phosphorous rich oxide was removed by deglazing HF etch, followed by a 200nm drive-in oxidation, used to drive the diffused phosphorous deeper into the substrate. This oxide layer was then removed by an HF wet etch and a 5nm thick layer of high-quality SiO_2 was grown by DCE-assisted (dichloroethylene) oxidation at 800C°. The Si-SiO_2 interface trap density was measured to be as low as $4x10^{10}$ cm^{-2} eV^{-1} using room temperature capacitance/voltage measurements.

The next processing step was the formation of nanoscale registration markers, used to provide crucial alignment of the subsequent fabrication steps. Arrays of registration markers (Fig. 1b), 100nm in size, were defined by electron beam lithography (EBL) in polymethyl-methacrylate (PMMA) resist and metallised using 15nm of Titanium followed by 65nm of Platinum. The markers were carefully engineered to withstand different processing steps and rapid thermal anneal (RTA) temperatures of 1000C°, used to activate the implanted donors. SEM images of registration markers before and after RTA are shown in Fig. 1 parts c and d. The measured accuracy of alignment, using the registration markers, was found to be within 25nm.

The last step, used to prepare the device for phosphorous ion implantation, was to define the EBL patterned implantation mask in 150nm thick layer of 950K molecular weight PMMA resist. The thickness of 150nm was chosen based on the SRIM modeling [8], which indicated a maximum ion penetration depth of 92nm, for this type of resist.

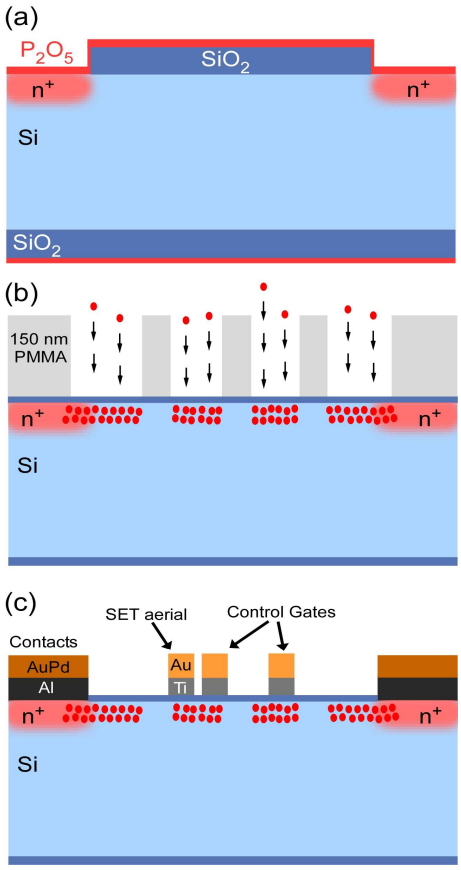

Fig. 2. Fabrication of the Si:P QCA cell: (a) Diffusion of n^+ contact regions; (b) Phosphorous ion implantation through an EBL-patterned PMMA resist mask; (c) Fabrication of the control gates and SETs on the surface of the SiO_2 layer.

Following the fabrication of the implantation mask, the QCA cell, consisting of four n+ islands (500 nm x 70 nm in size) with leads was defined by 14keV P+ phosphorus ion implantation, as shown in Fig. 2b. The tunnel barriers between the islands were effectively formed by the undoped near-intrinsic Si substrate between them. The tunneling barrier widths were set to ~ 60 nm to allow tunneling between adjacent dots and the respective reservoirs (within the two half-cells) while the separation between the half-cells was set to ~230 nm in order to suppress possible tunneling events. The implantation produced a doping density of n+ $\sim 10^{19}$ cm^{-3}, an order of magnitude above the metal-insulator transition. The mean implantation depth of the donors was found to be ~15 nm below the Si-SiO_2 interface [9]. A rapid thermal anneal at 1000C° for 5 seconds followed, used to repair the implant damage and to activate the donors.

After the implantation and the activation of the phosphorous donors, control and detection nanocircuitry was fabricated on the device surface (Fig. 2c), insulated from the implanted Si:P dots by the previously fabricated SiO_2 layer. Control gates, used to manipulate the electrostatic potential on the implanted islands, and the SET aerials, used to provide sufficient coupling between the islands and the subsequently fabricated SETs, were fabricated first. They were defined by standard EBL/liftoff technique using 60nm thick layer of 950K molecular weight PMMA and metalized in 10nm of titanium followed by 20nm of gold. Using the previously fabricated registration markers, the gates and the SET aerials were aligned to the implanted cell. This was followed by the formation of Al/AuPd ohmic contacts for QCA cell leads, defined using photolithography.

The last step in the process was the fabrication of the Aluminium readout SETs by double-angle evaporation through an EBL patterned suspended bi-layer resist mask [10]. The bi-layer resist consisted of 480nm of 33% PMMA-MAA copolymer and 50nm of 2.2M PMMA. The two Al evaporation steps were interrupted by a controlled oxidation step which formed the ~1nm thick AlO_x tunneling barrier in the SETs. The SET design was such that the SET islands were in direct contact with the aerials fabricated previously, as shown in Fig. 1a, ensuring a good capacitive coupling to the implanted islands of the QCA cell. After the completion of the fabrication process, the devices were individually inspected by SEM imaging combined with room temperature resistance characterization of each of the SETs to ensure operation at low (mK) temperatures.

3 ELECTRICAL MEASUREMENTS

Preliminary electrical measurements were performed in a dilution refrigerator operated at a base temperature of ~50mK. Magnetic field of 0.5 Tesla was applied throughout the measurements, in order to suppress the superconductivity of the aluminium. Both source and drain leads of both half-cells were grounded. The SETs were operated as sensitive charge detectors [6] by applying compensating voltages to their respective bias gates in order to counter the electrostatic potential changes on the SET islands induced by the variations of control gate voltages applied. Throughout the measurements, both SETs were biased on the descending sides of their Coulomb oscillation peaks, in order to distinguish the direction of electron transfers detected [11].

To characterize the device, the two half-cell electron occupancy state spaces were measured by sweeping the control gate voltages of each half-cell and monitoring the conductance of the respective SET [12]. The measurements showed clear honeycomb structures, characteristic of double dot systems. The data obtained was stable over time, enabling accurate biasing within the individual electron occupancy states of the two half-cells. This type of biasing was used to determine if the two half-cells are capacitivelly coupled, an essential requirement for QCA operation. This was done by repeatedly driving the half-cell A from the electron occupancy state (n_A, m_A) to state (n_A+1, m_A-1), using appropriate control gate voltages, while changing the biasing polarization of the opposite half cell in small steps from state (n_B, m_B) to state (n_B-1, m_B+1) [13]. The state of the half-cell A was being continuously monitored by measuring the conductance of the SET-A. Figure 3 shows the normalized induced charge on the island of SET-A as a function of the diagonal voltages V_A and V_B, applied to the two half-cells. If there was no capacitive coupling between the half-cells, the locus of the transition, between the two states in half-cell A, would be a straight line, being a linear combination of the two voltages V_A and V_B. The data, on the other hand, reveals a 'kink' which is a result of the charge rearrangement in half-cell B. To be precise, the electron transfer, in half-cell A, happens at different values of V_A, depending on the charge state the half-cell B is in, thus proving the existence of capacitive interaction between the two.

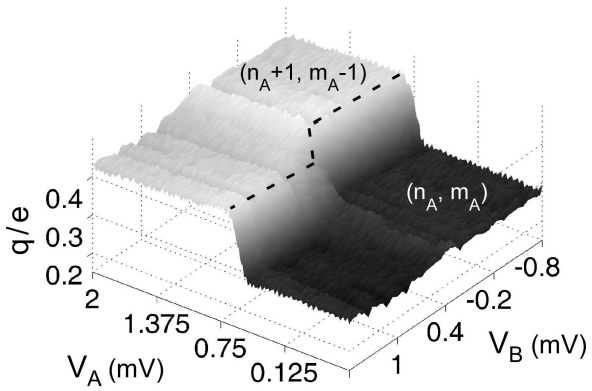

Fig. 3. The normalized charge induced on the island of SET-A as a function of the diagonal control gate voltages V_A and V_B applied to the two half-cells. The state transition in half-cell A reveals a 'kink' due to the capacitive coupling between the two half-cells.

4 CONCLUSIONS AND FUTURE WORK

We have developed and demonstrated a reproducible method for fabricating phosphorous ion implanted silicon QCA cells. The implantation was done using a $^{31}P^{+}$ ion beam, while nanoscale positioning was achieved using an EBL-patterned PMMA resist mask. Alignment accuracy of 25nm was realized using carefully engineered registration markers. The fabrication techniques used to create the cell are CMOS compatible with a great potential for down-scaling, possibly leading to single-donor QCA cells.

Preliminary measurements of these devices demonstrate capacitive coupling between the two half-cells, a very important result in the development of Si:P QCA. The next possible step in research is to attempt direct demonstration of QCA operation and to determine the range of conditions necessary for correct operation.

ACKNOWLEDGEMENTS

The authors would like to thank G.L. Snider for helpful discussions. This work was supported by the Australian Research Council, the Australian Government, and the US National Security Agency (NSA), Advanced Research and Development Activity (ARDA), and the Army Research Office (ARO) under contract number DAAD19-01-1-0653.

REFERENCES

[1] C. S. Lent, P. D. Tougaw, W. Porod, and G. H. Bernstein, Nanotechnology 4, 49, 1993.
[2] A. O. Orlov, I. Amlani, G. H. Bernstein, C. S. Lent, and G. L. Snider, Science 277, 928, 1997.
[3] R. P. Cowburn and M. E. Welland, Science 287, 1466, 2000.
[4] S. Gardelis, C. G. Smith, J. Cooper, D. A. Ritchie, E. H. Linfield, and Y. Jin, Phys. Rev. B 67, 033302, 2003.
[5] J. H. Cole, A. D. Greentree, C. J. Wellard, L. C. L. Hollenberg, and S. Prawer, Phys. Rev. B 71, 115302, 2005.
[6] M. H. Devoret and R. J. Schoelkopf, Nature 406, 1039, 2000.
[7] V. C. Chan, T. M. Buehler, A. J. Ferguson, D. R. McCamey, D. J. Reilly, A. S. Dzurak, R. G. Clark, C. Yang, and D. N. Jamieson, submitted to Appl. Phys. Lett. (2006).
[8] Software package SRIM.org: J.F. Ziegler, J.P. Biersack, U. Littmark, The Stopping and Range of Ions in Solids, Pergamon Press, 1985.
[9] D. N. Jamieson, C. Yang, T. Hopf, S. M. Hearne, C. I. Pakes, S. Prawer, M. Mitic, E. Gauja, S. E. Andresen, F. E. Hudson, A. S. Dzurak, and R. G. Clark, Appl. Phys. Lett. 86, 202101, 2005.
[10] T. A. Fulton and G. J. Dolan, Phys. Rev. Lett. 59, 109, 1987.
[11] T. M. Buehler, D. J. Reilly, R. Brenner, A. R. Hamilton, A. S. Dzurak, and R. G. Clark, Appl. Phys. Lett. 82, 577, 2003.
[12] M. Mitic, M. C. Cassidy, K. D. Petersson, R. P. Starrett, E. Gauja, R. Brenner, C. Yang, D. N. Jamieson, R. G. Clark, and A. S. Dzurak, to be submitted to Appl. Phys. Lett. (2006).
[13] W. Porod, C. S. Lent, G. H. Bernstein, A. O. Orlov, I. Amlani, G. L. Snider, and J. L. Merz, Int. J. Electronics, 86, 549-590, 1999.